

Effect of running coupling on photons from jet - plasma interaction in relativistic heavy ion collisions

Lusaka Bhattacharya* and Pradip Roy†
Saha Institute of Nuclear Physics, Kolkata - 700064, India

We discuss the role of collisional energy loss on high p_T photon data measured by PHENIX collaboration by calculating photon yield in jet-plasma interaction. The phase space distribution of the participating jet is dynamically evolved by solving Fokker-Planck equation. We treat the strong coupling constant (α_s) as function of momentum and temperature while calculating the drag and diffusion coefficients. It is observed that the quenching factor is substantially modified as compared to the case when α_s is taken as constant. It is shown that the data is reasonably well reproduced when contributions from all the relevant sources are taken into account. Predictions at higher beam energies relevant for LHC experiment have been made.

PACS numbers:

Keywords: energy-loss, quark-gluon-plasma

I. INTRODUCTION

Heavy ion collisions have received significant attention in recent years. Various possible probes have been studied in order to detect the signatures of quark gluon plasma (QGP). Study of direct photon and dilepton spectra emanating from hot and dense matter formed in ultra-relativistic heavy ion collisions is a field of considerable current interest. Electromagnetic probes have been proposed to be one of the most promising tools to characterize the initial state of the collisions [1]. Because of the very nature of their interactions with the constituents of the system they tend to leave the system almost unscattered. In fact, photons (dilepton as well) can be used to determine the initial temperature, or equivalently the equilibration time. These are related to the final multiplicity of the produced hadrons in relativistic heavy ion collisions (HIC). By comparing the initial temperature with the transition temperature from lattice QCD, one can infer whether QGP is formed or not.

Photons are produced at various stages of the evolution process. The initial hard scatterings (Compton and annihilation) of partons lead to photon production which we call hard photons. If quark gluon plasma (QGP) is produced initially, there are QGP-photons from thermal Compton plus annihilation processes. Photons are also produced from different hadronic reactions from hadronic matter either formed initially (no QGP scenario) or realized as a result of a phase transition (assumed to be first order in the present work) from QGP. In addition to that there is a large background of photons coming from π^0 and η^0 decays. If this decay contribution is subtracted from the total photon yield what is left is the direct (excess) photons.

These apart, there exists another class of photon emission process via the jet conversion mechanism (jet-plasma

interaction) [2] which occurs when a high energy jet interacts with the medium constituents via annihilation and Compton processes. It might be noted that this phenomenon (for Compton process) has been illustrated quite some time ago [3] in the context of estimating photons from equilibrating plasma. There, it is assumed that because of the larger cross-section, gluons equilibrate faster providing a heat bath to the incoming quark-jet. A comparison of the non-equilibrium photons (equivalent to photons from jet-plasma interaction) with the direct photons (thermal) shows that this contribution remains dominant for photons with p_T upto 6 GeV. However, while evaluating jet-photon the authors in Ref. [2] assumes that the largest contribution to photons corresponds to $p_\gamma \sim p_q(p_{\bar{q}})$. This implies that the annihilating quark (anti-quark) directly converts into a photon. In the present work, we calculate photons from jet-plasma interaction relaxing the above assumption and including the energy loss of the participating jet where the strong coupling constant (α_s) is taken as 'running' as given in Ref. [4].

The phenomena of jet quenching vis-a-vis energy loss have been studied by several authors [5] taking into account both collisional and radiative losses. However, in the present work, our main concern is to examine the role of collisional loss (where α_s is running) in the context of photon production from jet-plasma interaction for the following reason. The suppression of single electron data [6] is more than expected which led to the re-thinking of the importance of collisional energy loss in the context of RHIC data. A substantial amount of work has been done to look into this issue in recent times [4, 7–11]. Few comments about the recent developments of collisional energy loss are in order here. It is argued in Ref. [12] that the collisional energy loss is approximately of the same order as the radiative loss. It is also shown by Braun et. al [4] that the collisional energy loss increases substantially if the strong coupling is treated as function of temperature and momentum and if, in addition to t -channel process, the inverse Compton reaction is considered. In a most recent calculation, using a reduced

*Electronic address: lusaka.bhattacharya@saha.ac.in

†Electronic address: pradipk.roy@saha.ac.in

screening mass and running coupling the collisional energy loss is six times larger than that with the constant coupling [13]. It explains single electron R_{AA} quite well. However, it fails to account for the elliptic flow, v_2 of the electron. Effective resonance with LO-pQCD model [14] also improves the collisional energy loss and the single electron data is well reproduced. It is also important to note that only the radiative energy loss fails to account for the single electron data at RHIC [15]. On the other hand, the authors of Ref. [16] claims that the collisional energy loss is sub-leading. However, in order to see the effects of energy loss on jet-photon one should also incorporate the radiative energy loss for completeness and this has to be done in the same formalism in a realistic scenario.

Thus, it is apparent that the issue of the relative importance of the mechanism of energy loss in the context of RHIC data is not settled yet. We shall re-visit the importance of collisional energy loss in the context of photons from jet-plasma interactions. Moreover, in high temperature (T) effective field theory the coupling constant, α_s , is taken to be a function of temperature only, which may be justified when $T \gg \Lambda_{\text{QCD}}$. However, in the case of relativistic heavy ion collisions, temperature is not the only scale, there is the momentum scale (k) also. One has to take into account the case when $k \sim T$ and treat α_s to be function of both k and T [4]. By incorporating this fact it is shown that the energy loss is by a factor of 2–4 more than the case when α_s is constant. It is for this purpose we concentrate on the collisional energy loss [7, 17] with the formalism given in Ref. [4] to calculate photons from jet-plasma interaction. For completeness, we also include the radiative loss in an effective way.

The organization of the paper is as follows. We give a brief description of jet-photon production in QGP in section II A. The evolution of jet quark and photon p_T distributions are discussed in sections II B and II C respectively. Section III is devoted to the discussions of results and finally, we summarize in section IV.

II. FORMALISM

A. Jet-Photon Rate

The lowest order processes for photon emission from QGP are the Compton scattering ($q(\bar{q})g \rightarrow q(\bar{q})\gamma$) and annihilation ($q\bar{q} \rightarrow g\gamma$) process. The total cross-section diverges in the limit t or $u \rightarrow 0$. These singularities have to be shielded by thermal effects in order to obtain infrared safe calculations. It has been argued in Ref. [18] that the intermediate quark acquires a thermal mass in the medium, whereas the hard thermal loop (HTL) approach of Ref. [19] shows that very soft modes are suppressed in a medium providing a natural cut-off $k_c \sim gT$. We assume that the singularities can be shielded by the introduction of thermal masses for the

participating partons. Apart from the thermal interactions of the plasma partons, interaction of a leading jet parton with the plasma was found to be a very important source of photons.

The differential photon production rate for this process is given by:

$$E \frac{dR}{d^3p} = \frac{\mathcal{N}}{2(2\pi)^3} \int \frac{d^3p_1}{2E_1(2\pi)^3} \frac{d^3p_2}{2E_2(2\pi)^3} \frac{d^3p_3}{2E_3(2\pi)^3} f_{jet}(\mathbf{p}_1) \times f_2(E_2)(2\pi)^4 \delta(p_1 + p_2 - p_3 - p) |\mathcal{M}|^2 (1 \pm f_3(E_3)) \quad (1)$$

where, $|\mathcal{M}|^2$ represents the spin averaged matrix element squared for one of those processes which contributes in the photon rate and \mathcal{N} is the degeneracy factor of the corresponding process. f_{jet} , f_2 and f_3 are the initial state and final state partons. f_2 and f_3 are the Bose-Einstein or Fermi-Dirac distribution functions.

$$f_2(E_{2,3}) = \frac{1}{\exp(E_{2,3}/kT) \pm 1} \quad (2)$$

B. Fokker - Planck Equation: Parton transverse momentum spectra

In the photon production rate (from jet-plasma interaction) one of the collision partners is assumed to be in equilibrium and the other (the jet) is executing random motion in the heat bath provided by quarks (anti-quarks) and gluons. Furthermore, the interaction of the jet is dominated by small angle scattering. In such scenario the evolution of the jet phase space distribution is governed by Fokker-Planck (FP) equation where the collision integral is approximated by appropriately defined drag and diffusion coefficients.

As mentioned already in the introduction that the quark jet here is not in equilibrium. Therefore the corresponding distribution function (f_{jet}) that appears in Eq. (1) is calculated by solving the FP equation. The energy loss is represented by the drag coefficient (see later). The FP equation, can be derived from Boltzmann equation if one of the partners of the binary collisions is in thermal equilibrium and the collisions are dominated by the small angle scattering involving soft momentum exchange [8, 14, 20–24]. For a longitudinally expanding plasma, FP equation reads [8, 25]:

$$\left(\frac{\partial}{\partial t} - \frac{p_z}{t} \frac{\partial}{\partial p_z} \right) f(\mathbf{p}_T, p_z, t) = \frac{\partial}{\partial p_i} A_i(\mathbf{p}) f(\mathbf{p}) + \frac{1}{2} \frac{\partial}{\partial p_i \partial p_j} [B_{ij}(\mathbf{p}) f(\mathbf{p})], \quad (3)$$

where [8]

$$A_i = \frac{\nu}{16p(2\pi)^5} \int \frac{d^3k'}{k'} \frac{d^3k}{k} \frac{d^3q}{q'} d\omega q_i |\mathcal{M}|_{t \rightarrow 0}^2 f(k)(1 + f(k')) \delta^3(\mathbf{q} - \mathbf{k}' + \mathbf{k}) \delta(\omega - \mathbf{v}_{\mathbf{k}'} \cdot \mathbf{q}) \delta(\omega - \mathbf{v}_{\mathbf{k}} \cdot \mathbf{q}) \quad (4)$$

$$B_{ij} = \frac{\nu}{16p(2\pi)^5} \int \frac{d^3k'}{k'} \frac{d^3k}{k} \frac{d^3q}{p'} d\omega q_i q_j |\mathcal{M}|_{t \rightarrow 0}^2 f(k) \times (1 + f(k')) \delta^3(\mathbf{q} - \mathbf{k}' + \mathbf{k}) \delta(\omega - \mathbf{v}_{\mathbf{k}'} \cdot \mathbf{q}) \delta(\omega - \mathbf{v}_{\mathbf{k}} \cdot \mathbf{q}), \quad (5)$$

Here ν is the appropriate degeneracy factor. Note that the coefficient A_i is related the drag coefficient η by $A_i = \eta p_i$, where $\eta = (1/E)dE/dx$.

Now, B_{ij} can be decomposed into longitudinal and transverse components:

$$B_{ij} = B_t (\delta_{ij} - \frac{p_i p_j}{p^2}) + B_l \frac{p_i p_j}{p^2} \quad (6)$$

Explicit calculation shows that the off diagonal components of B_{ij} vanish and we have,

$$B_{t,l} = \frac{\nu}{(2\pi)^4} \int \frac{d^3k d^3q d\omega}{2k 2k' 2p 2p'} \delta(\omega - \mathbf{v}_{\mathbf{p}} \cdot \mathbf{q}) \delta(\omega - \mathbf{v}_{\mathbf{k}} \cdot \mathbf{q}) \langle \mathcal{M} \rangle_{t \rightarrow 0}^2 f(k) [1 + f(k) + \omega \frac{\partial f}{\partial k}] q_{t,l}^2, \quad (7)$$

where, $B_l = d\langle(\Delta p_z)^2\rangle/dt$, $B_t = d\langle(\Delta p_T)^2\rangle/dt$, represent diffusion constants along parallel and perpendicular directions of the propagating partons. Evidently, A_i ($B_{t,l}$) is infrared singular. Such divergences do not arise if close and distant collisions are treated separately. For very low momentum transfer the concept of individual collision breaks down and one has to take collective excitations of the plasma into account. Hence there should be a lower momentum cut off above which bare interactions might be considered. While for soft collisions medium modified hard thermal loop corrected propagator should be used [7, 26]. It is evident that Eq. (4) actually gives dE/dt or the energy loss rate [7] that can be related to the drag coefficient.

However, in the above treatment, the infra-red cut-off is fixed by plasma effects, where only the medium part is considered, completely neglecting the vacuum contribution leading to ambiguity in the energy loss calculation. If the latter part is taken into account the strong coupling should be running. Thus for any consistent calculation one has to take into consideration this fact. In that case $\alpha_s = \alpha_s(k, T)$ ($k = \sqrt{|\omega^2 - q^2|}$ in this case), and the above integrals must be evaluated numerically where the infra-red cut-off is fixed by Debye mass to be solved self-consistently:

$$m_D(T) = 4\pi \left(1 + \frac{N_F}{6}\right) \alpha_s(m_D(T), T) T^2 \quad (8)$$

We reiterate that the matrix elements in Eqs. (4) and (7) contains the strong coupling which we take as running, i. e. $\alpha_s = \alpha_s(\sqrt{|\omega^2 - q^2|}, T)$. We chose the following parameterization of α_s which respects the perturbative ultra-violet (UV) behavior and the 3D infra-red (IR) point [4]:

$$\alpha_s(k, T) = \frac{u_1 \frac{k}{T}}{1 + \exp(u_2 \frac{k}{T} - u_3)}$$

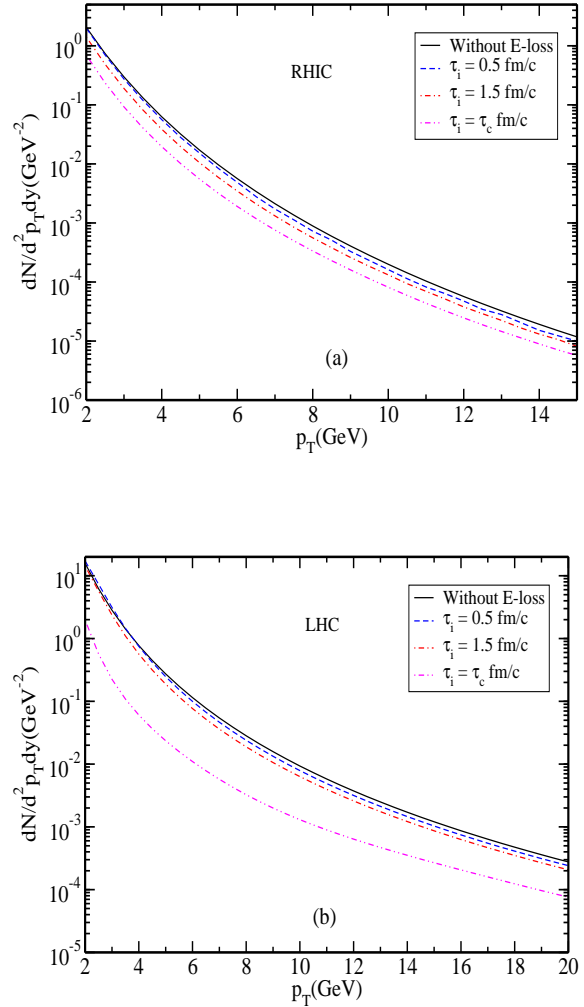


FIG. 1: (Color online) p_T distribution of parton at (a) RHIC energy ($T_i = 0.446$ GeV and $\tau_i = 0.147$ fm/c) and at (b) LHC energy ($T_i = 0.897$ GeV, $\tau_i = 0.073$ fm/c).

$$+ \frac{v_1}{(1 + \exp(v_2 \frac{k}{T} - v_3))(\ln(e + (\frac{k}{\lambda_s})^a + (\frac{k}{\lambda_s})^b))}, \quad (9)$$

with $k = \sqrt{|\omega^2 - q^2|}$ in this case. The parameters a , b and λ_s are given by $a = 9.07$, $b = 5.90$ and $\lambda_s = 0.263$ GeV. For the limiting behavior ($k \ll T$) of the coupling we choose,

$$u_1 = \alpha_{3d}^*(1 + \exp(-u_3)) \quad (10)$$

Here α_{3d}^* and α_s^* denote the values of the IR fixed point of $SU(3)$ Yang-Mills theory in $d = 3$ and $d = 4$ dimensions, respectively. The remaining four parameters ($u_2 = 5.47$, $u_3 = 6.01$, $v_2 = 10.13$ and $v_3 = 9.27$) fit the numerical results for pure Yang-Mills theory obtained from the RG equations in Ref. [27].

So far we have discussed about the collisional energy loss which, although, dominates at lower energies, is not the only mechanism of energy loss. As the energy increases radiative energy loss starts to dominate and hence

cannot be neglected. In case of jet-photon production, since the photon energy is almost equal to the jet energy, one has to include the radiative loss to account for the high p_T photons. However, in order to see the effects of both the collisional and radiative energy losses, one must develop a formalism in which both the mechanisms can be taken into account in a consistent manner. The two mechanisms are not entirely independent, i.e., the collisional loss may influence the radiative loss. Thus both should be included to calculate transport coefficients. Since there is no rigorous way to implement this, the approximate way is to define effective drag (diffusion) in the following manner:

$$\begin{aligned} \eta &= \eta_{\text{coll}} + \eta_{\text{rad}} \\ &= \frac{1}{E} \left[\left(\frac{dE}{dx} \right)_{\text{coll}} + \left(\frac{dE}{dx} \right)_{\text{rad}} \right] \end{aligned} \quad (11)$$

where $\left(\frac{dE}{dx} \right)_{\text{coll}}$ can be calculated from Eq. (4) keeping in mind that $\eta p_i = A_i$. The collisional (differential) energy loss $(dE/dx)_{\text{coll}}$ can be calculated from Eq. (4) using the method described in [8]. For running α_s it is given by,

$$\left(\frac{dE}{dx} \right)_{\text{coll}} = \frac{4}{3} \pi \left(1 + \frac{N_f}{6} \right) T^2 \int_{m_D^2}^s dt |t| \frac{\alpha_s^2(\sqrt{|t|}, T)}{|t|^2} |t| \quad (12)$$

Where, $s = 2ET$, E is the energy of the incident quark. The radiative energy loss is given by,

$$\left(\frac{dE}{dx} \right)_{\text{rad}} = \frac{C_F \alpha_s(E, T)}{N(E)} \frac{L \mu^2}{\lambda_g} \ln\left(\frac{E}{\mu}\right), \quad (13)$$

where $N(E)$ is an energy dependent factor and $N(E \rightarrow \infty) = 4$ if kinematic bounds are neglected [28]. It is important to point out here that $N(E) = 7.3, 10.1, 24.4$ for $E = 500, 50, 5$ GeV respectively and $N(E \rightarrow \infty) = 4$ (see the Ref. [28]). L is the distance traversed by the jets in the plasma. Similarly we can define the effective diffusion coefficients.

Having known the drag and diffusion, we solve the FP equation using Green's function techniques: If $P(\vec{p}, t | \vec{p}_0, t_i)$ is a solution to Eq. (3) with the initial condition

$$P(\vec{p}, t = t_i | \vec{p}_0, t_i) = \delta^{(3)}(\vec{p} - \vec{p}_0) \quad (14)$$

the full solution with an arbitrary initial condition can be obtained as [22]

$$f(t, \vec{p}) = \int d^3 \vec{p}_0 P(\vec{p}, t | \vec{p}_0, t_i) f_0(\vec{p}_0) \quad (15)$$

where for the initial condition $f(t = 0, \vec{p}) = f_0(\vec{p}_0)$ and $P(\vec{p}, t | \vec{p}_0, t_i)$ is the Green's function of the partial differential Eq. (2).

We assume here that the plasma expands only longitudinally (Bjorken expansion scenario [29]). The reason is the following. The transverse expansion will have

two effects on the parton energy loss: (i) The expanding geometry will increase the duration of propagation, (ii) the same expansion will cause the parton density to fall along its path. These two effects partially compensate each other and the energy loss is almost the same as in the case without transverse expansion [30]. Since we are considering the central rapidity region ($|\eta| < 0.35$) the arguments given above is not applicable in the case of longitudinal expansion scenario.

The solution with an arbitrary initial momentum distribution can now be written as [14],

$$E \frac{dN}{d^3 p} = \int d^3 p_0 P(\vec{p}, t | \vec{p}_0, t_i) E_0 \frac{dN}{d^3 p_0} \quad (16)$$

We use the initial parton p_T distributions (at the formation time t_i) taken from [2, 31]:

$$\frac{dN}{d^2 p_0 T dy_0} \Big|_{y_0=0} = \frac{K N_0}{(1 + \frac{p_{0T}}{\beta})^\alpha}, \quad (17)$$

where K is a phenomenological factor ($\sim 1.5 - 2$) which takes into account the higher order effects. The values of the parameters are listed in Table. I. We note that the

	RHIC		LHC	
	q	\bar{q}	q	\bar{q}
N_0 [1/GeV 2]	5.0×10^2	1.3×10^2	1.4×10^4	1.4×10^5
β [GeV]	1.6	1.9	0.61	0.32
α	7.9	8.9	5.3	5.2

TABLE I: Parameters for initial parton p_T distribution.

parametric form of Eq. (17) may not represent the true picture of the jet p_T distribution. In recent years, more sophisticated calculations have been done using different parameterizations of the parton distribution functions. The p_T distribution used here might differ substantially from these calculations and the results presented here is correct upto a factor that might come from using the more state of the art calculation.

C. Space time evolution

In order to obtain the space-time integrated rate we first note that the phase space distribution function for the incoming jet in the mid rapidity region is given by (see Ref. [32] for details)

$$\begin{aligned} f_{jet}(\vec{r}, \vec{p}, t') \Big|_{y=0} &= \frac{(2\pi)^3 \mathcal{P}(|\vec{w}_r|) t_i}{\nu_q \sqrt{t_i^2 - z_0^2}} \frac{1}{p_T} \\ &\times \frac{dN}{d^2 p_T dy} (p_T, t') \delta(z_0) \end{aligned} \quad (18)$$

where $\frac{dN}{d^2 p_T dy}(p_T, t')$ can be obtained from Eq. (16). t_i is the jet formation time and ν_q is the spin-color degeneracy

factor. z_0 is the jet formation position in the direction of QGP expansion and $\mathcal{P}(|\vec{w}_r|)$ is the initial jet production probability distribution at the initial radial position \vec{w}_r in the plane $z_0 = 0$, where

$$|\vec{w}_r| = (\vec{r} - (t' - t_i) \frac{\vec{p}}{|\vec{p}|}) \cdot \hat{r}$$

$$= \sqrt{(r \cos \phi - t')^2 + r^2 \sin^2 \phi} \quad \text{for } t_i \sim 0 \quad (19)$$

and ϕ is the angle in the plane $z_0 = 0$ between the direction of the photon and the position where this photon has been produced. We assume the plasma expands only longitudinally. Thus using $d^4x = r dr dt' d\phi dz$ and the expression for f_{jet} from Eq. 17 we obtain the transverse momentum distribution of photon as follows [32, 33]:

$$\frac{dN^\gamma}{d^2p_T dy} = \int d^4x \frac{dN^\gamma}{d^4x d^2p_T dy}$$

$$= \frac{(2\pi)^3}{\nu_q} \int_{t_i}^{t_c} dt' \int_0^R r dr \int d\phi \mathcal{P}(\vec{w}_r)$$

$$\times \frac{\mathcal{N}_i}{16(2\pi)^7 E_\gamma} \int d\hat{s} d\hat{t} |\mathcal{M}_i|^2 \int dE_1 dE_2$$

$$\times \frac{1}{p_{1T}} \frac{dN}{dp_{1T}^2 dy} (p_{1T}, t') \frac{f_2(E_2)(1 \pm f_3(E_3))}{\sqrt{aE_2^2 + 2bE_2 + c}} \quad (20)$$

f_{jet} is the distribution function of the jet quark (see Eq. (18)) and rest of the distribution functions i.e f_2, f_3 are Fermi-Dirac or Bose-Einstein distributions. ϕ dependence occurs only in $\mathcal{P}(\vec{w}_r)$. So the ϕ integration can be done analytically as in Ref. [32]. The temperature profile is taken from Ref. [32].

Besides the thermal photons from QGP and hadronic matter we also calculate photons from initial hard scattering from the reaction of the type $h_A h_B \rightarrow \gamma X$ using perturbative QCD. We include the transverse momentum broadening in the initial state partons [34, 35]. The cross-section for this process can then be written in terms of elementary parton-parton cross-section multiplied by the partonic flux which depends on the parton distribution functions (PDF) for which we take CTEQ parameterization [36]. A phenomenological factor K is used to take into account the higher order effects. We also include photons from fragmentation process.

III. RESULTS

To obtain the quark momentum distribution we use Eqs. (3), (4), (7), (8) and (16). The transverse momentum distributions of quarks are shown in Fig. 1 for different times (proper) at RHIC and LHC energies respectively where the initial distributions are taken from Eq. (17). It is observed that the spectra are more reduced as the time increases. It is generally assumed that quarks fragment into hadrons around τ_c (the begining of

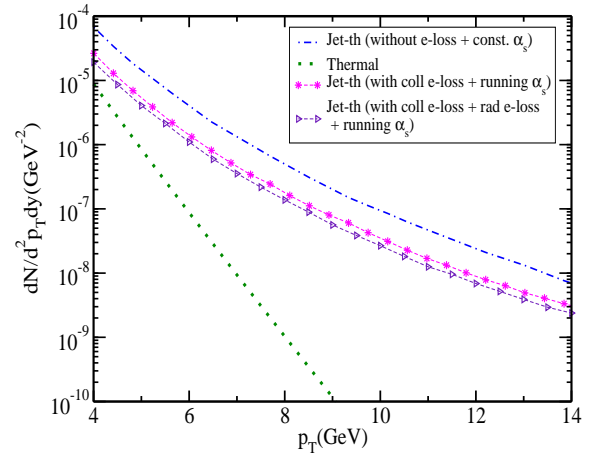


FIG. 2: (Color online) p_T distribution of photons at RHIC energy with $T_i = 0.446$ GeV and $\tau_i = 0.147$ fm/c. The violet (magenta) curve denotes the photon yield from jet-plasma interaction with collisional (collisional + radiative) energy loss. The blue curve corresponds to the case without any energy loss and the green curve represents the thermal contribution.

the hadronic phase) where the quenching factor is the largest. At LHC energies (see Fig. 1b) this factor is more as the temperature in this case is large compared to RHIC energies. It is seen from Eq. (20) the photon p_T distribution is directly proportional to the quark p_T spectra. Thus the photon yield will be affected as we shall see in the following.

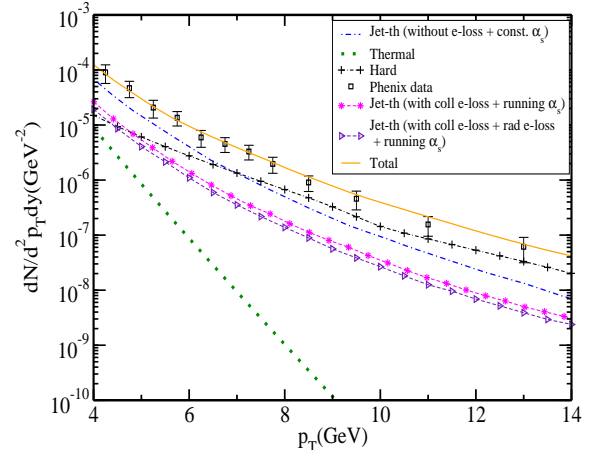


FIG. 3: (Color online) p_T distribution of photons at RHIC energy with $T_i = 0.446$ GeV and $\tau_i = 0.147$ fm/c. The magenta (blue) curve denotes the photon yield from jet-plasma interaction running (constant) α_s . The black (green) curve corresponds to hard (thermal) photons. The orange represents the total photon yield compared with the Phenix measurements of photon data [37].

In order to obtain the photon p_T distribution we numerically integrate Eq. (20) using Eq. (16). The results for jet-photons for RHIC energies are plotted in Fig. 2

where we have taken $T_i = 446$ MeV and $t_i = 0.147$ fm/c. As indicated earlier, the radiative energy loss starts dominating at higher energies of the jet, we include this in the calculation of photon p_T distribution. We find that the yield is decreased with the inclusion of both the energy loss mechanisms as compared to the case when only collisional energy loss is considered. It is to be noted that when one considers collisional energy loss alone the yield with constant α_s is more compared to the situation when running α_s is taken into account. This is due to the fact that the energy loss in the later case is more [4]. On the other hand, with the inclusion of the radiative loss the yield decreases further.

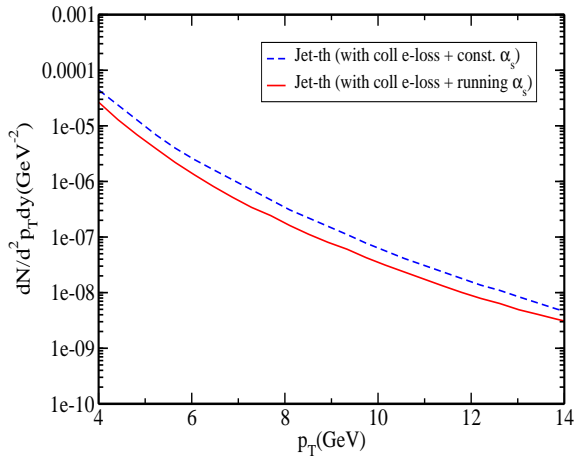


FIG. 4: (Color online) p_T distribution of jet-th photons at RHIC energy with $T_i = 0.446$ GeV and $\tau_i = 0.147$ fm/c. The red (blue) curve denotes the photon yield coming from jet-plasma interaction with collisional energy loss + running (constant) α_s .

In order to compare our results with high p_T photon data measured by the PHENIX collaboration [37], we have to evaluate the contributions to the photons from other sources, that might contribute in this p_T range. In Fig. 3 the results for jet-photons corresponding to the RHIC energies are shown, where we have taken $T_i = 446$ MeV and $t_i = 0.147$ fm/c. The individual contributions from hard and bremsstrahlung processes [38] are also shown for comparison. These are estimated using the formalism given in Ref. [38]. The total yield comprises of photons from jet-plasma interaction (with energy loss), hard and bremsstrahlung processes, thermal Compton and annihilation processes. We also show in a separate plot (in Fig. 4) photons from jet-plasma interaction corresponding to the cases with constant α_s and running α_s with collisional energy loss alone. It is observed that the spectra in the case of collisional energy loss with running coupling is depleted by a factor 1.7 – 2 compared to the case where the strong coupling is constant. This is expected as the energy loss is more in the

former case. The yield further reduces when both the mechanisms of energy loss are included. The total photon yield consisting of jet-photon, photons from initial hard collisions, jet-fragmentation and thermal photons is compared with the PHENIX photon data [37]. It is seen that the data is well reproduced in our model (see Fig. 3). To cover the uncertainties in the initial condi-

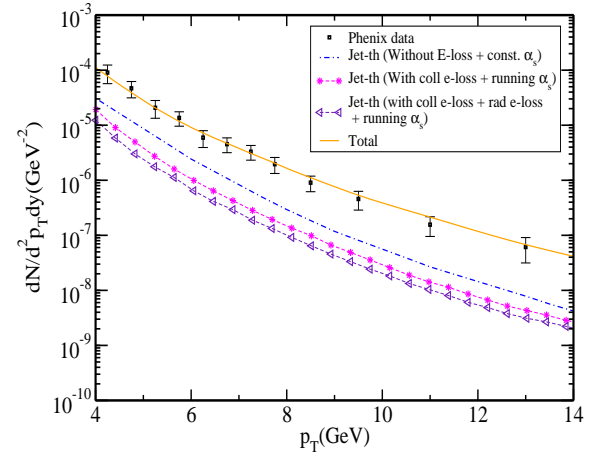


FIG. 5: (Color online) p_T distribution of photons at RHIC energies with $T_i = 0.350$ GeV and $\tau_i = 0.25$ fm/c. The orange line corresponds to total photon yield from all the sources as in Fig. 3 with both energy losses (collisional + radiative) included in the jet-photon contribution.

tions for a given beam energy, we consider another set of initial conditions at a lower temperature $T_i = 0.350$ GeV and somewhat later initial time of $\tau_i = 0.25$ fm/c. The yield for this set is shown in Fig. 5. We see that the data is reproduced reasonably well.

In Fig. 6 we plot the p_T distribution of photons for the RHIC energy ($T_i = 0.236$ GeV and $\tau_i = 0.5$ fm/c) for a lower value of $dN/dy = 600$. It is clearly visible from Fig. 6 that we can not explain Phenix photon data satisfactorily in the p_T range 4 – 8 GeV. For the higher p_T range Phenix photon data is well reproduced.

We also consider the high p_T photon production at LHC energies. The contributions from various sources are shown in Figs. 7 where the jet-plasma contribution is calculated with running coupling constant (α_s) (considering both the collisional and radiative energy losses). Since the initial temperature in this case is higher, the plasma lives for longer time. Thus the energy loss suffered by the parton is more. As a result, the difference between the cases with and without energy loss is slightly more than what is obtained at RHIC. It is observed that due to the inclusion of radiative energy loss along with collisional energy loss the jet photon yield is suppressed significantly. Also due to the inclusion of running coupling constant the jet photon yield is suppressed by a factor of 3 – 4.

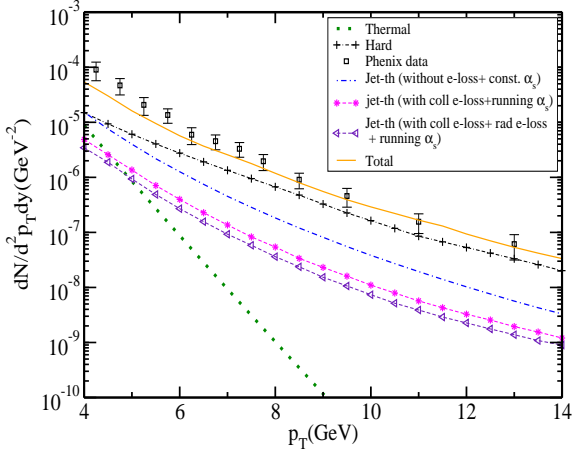


FIG. 6: (Color online) p_T distribution of photons at RHIC energy with $T_i = 0.236$ GeV and $\tau_i = 0.5$ fm/c. The magenta (blue) curve denotes the photon yield from jet-plasma interaction running (constant) α_s . The black (green) curve corresponds to hard (thermal) photons. The orange represents the total yield compared with the Phenix measurements of photon data [37].

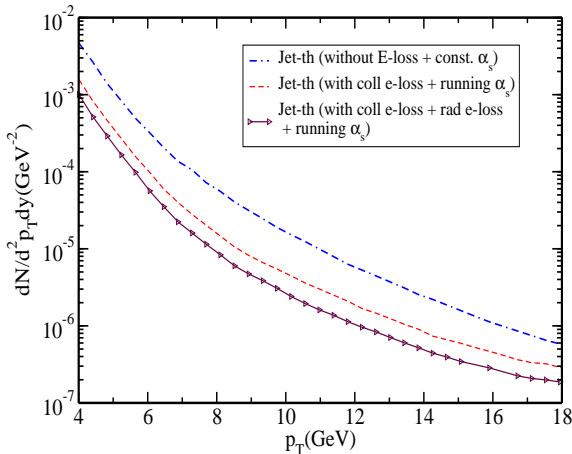


FIG. 7: (Color online) Same as Fig.(3) at LHC energy ($T_i = 0.897$ GeV and $\tau_i = 0.073$ fm/c).

IV. SUMMARY

We have calculated the transverse momentum distribution of photons from jet plasma interaction with running coupling, i. e. with $\alpha_s = \alpha_s(k, T)$ where we have included both collisional and radiative energy losses. It is found that the assumption made in Ref. [2] while calculating photons from jet-plasma interactions may not be good at LHC energies as we observe a difference is by a factor of 2–3. Using running coupling we find that the depletion in the photon p_T spectra is by a factor of 2–2.5 more as compared to the case with constant coupling for RHIC energies. This is due to the fact that the energy loss (and hence drag and diffusion coefficients) is more by similar factor in the case of running coupling. Phenix photon data have been contrasted with the present calculation and the data seem to have been reproduced well in the low p_T domain. The energy of the jet quark to produce photons in this range ($4 < p_T < 14$) is such that collisional energy loss plays important role here. It is shown that inclusion of radiative energy loss also describes the data reasonable well.

To check the sensitivity with the initial conditions, we consider two sets of initial conditions. In both the cases the data can be described quite well. This is due to the fact that both the initial conditions corresponds to the same $dN/dy = 1150$.

As we validate our model through the description of Phenix photon data we also predict the high p_T photon yield that might be expected in the future experiment at LHC. We notice that the inclusion of the radiative energy loss further reduces the yield at high p_T . It is observed that the contribution from jet-plasma interaction is slightly more reduced as compared to the RHIC case as the initial temperature is higher at LHC.

We do not consider transverse expansion as the energy loss of the partons remains just about the same as the case without transverse expansion. Finally, we conclude by noting that the role of running coupling constant should be explored in the context of other observables such as thermal photons, dileptons and so on.

[1] J. Alam, S. Sarkar, P. Roy, T. Hatsuda, and B. Sinha, Ann. Phys. **286** 159 (2000).
[2] R. J. Fries, B. Muller, and D. K. Srivastava, Phys. Rev. Lett. **90**, 132301 (2003).
[3] P. Roy, J. Alam, S. Sarkar, B. Sinha, and S. Raha, Nucl. Phys. A**624**, 687 (1997).
[4] J. Braun and H-J. Pirner, Phys. Rev. D**75**, 054031 (2007).
[5] J. D. Bjorken, Fermilab-Pub-82/59-THY(1982) and Erratum (Unpublished); M. Gyulassy, P. Levai and I. Vitev, Nucl. Phys. B **571**, 197 (2000); B. G. Zakharov, JETP Lett. **73**, 49 (2001); M. Djordjevic and U. Heinz, Phys. Rev. Lett **101**, 022302 (2008); R. Baier *et al.*, J. High Ener. Phys. **0109**, 033 (2001); S. Jeon and G. D. Moore, Phys. Rev. C**71**, 034901 (2005); A. K. Dutt-Mazumder, J. Alam, P. Roy, and B. Sinha, Phys. Rev. D **71**, 094016 (2005); P. Roy, J. Alam, and A. K. Dutt-Mazumder, J. Phys. G. **35**, 104047 (2008).
[6] S. S. Adler *et al.*, Phenix Collaboration, Phys. Rev. Lett. **96** 032301 (2006).
[7] A. K. Dutt-Mazumder, J. Alam, P. Roy, B. Sinha, Phys. Rev. D**71**, 094016 (2005).

- [8] P. Roy, A. K. Dutt-Mazumder and J. Alam, Phys. Rev. C**73**, 044911 (2006).
- [9] A. Adil, M. Gyulassy, W. Horowitz and S. Wicks, Phys. Rev. C**75** 044906 (2007); M. Djordjevic, Phys. Rev. C**74** 064907 (2006); T. Renk, Phys. Rev. C**76** 064905 (2007).
- [10] S. Peigne, P. B. Gossiaux, and T. Gousset, J. High Energy Phys. **04**, 011 (2006).
- [11] A. Ayala, J. Magnin, L. M. Montano, and E. Rojas, Phys. Rev. C**77**, 044904 (2008).
- [12] M. Gyulassy, I. Vitev, X. N. Wang, and B.W. Zhang, nucl-th/0302077.
- [13] P. B. Gossiaux and A. Aichelin, Phys. Rev. C**78**, 014904 (2008).
- [14] H. V. Hees and R. Rapp, Phys. Rev. C**71** 034907 (2005).
- [15] S. Wicks, W. Horowitz, M. Djordjevic, and M. Gyulassy, Nucl. Phys. A**784**, 426 (2007).
- [16] G -Y Qin, J. Ruppert, C. Gale, S. Jeon, G. Moore, and M. G. Mustafa, Phys. Rev. Lett **100**, 072301 (2008).
- [17] M. H. Thoma, Phys. Lett. B**273**, 128 (1991).
- [18] K. Kajantie and P. V. Russkanen Phys. Lett. B**121**, 352 (1983).
- [19] R. D. Pisarski and E. Braaten, Nucl. Phys. B**337**, 569 (1990); *ibid* Nucl. Phys. B**339**, 310 (1990).
- [20] J. Alam, S. Raha and B. Sinha, Phys. Rev. Lett **73**, 1895 (1994).
- [21] B. Svetitsky, Phys. Rev. D**37**, 2484 (1988).
- [22] G. D. Moore and D. Teaney, Phys. Rev. C**71**, 064904 (2005).
- [23] M. B. G. Ducati, V. P. Goncalves and L. F. Mackedanz, hep-ph/0506241.
- [24] J. BJORAKER and R. Venugopalan, Phys. Rev. C**63**, 024609 (2001).
- [25] G. Baym, Phys. Lett. B**138** 18 (1984).
- [26] M. H. Thoma and M. Gyulassy, Nucl. Phys. B**351**, 491(1991).
- [27] J. Braun and H. Gies, J. High energy Phys. **06** 024 (2006).
- [28] M. Gyulassy, P. Levai and I. Vitev, Nucl. Phys. B**571**, 197 (2000).
- [29] J. D. Bjorken, Phys. Rev. D**27** 140 (1983).
- [30] M. Gyulassy, I. Vitev, X. N. Wang, and P. Huovinen, Phys. Lett. B**526**, 301 (2002).
- [31] B. Muller, Phys. Rev. C**67** 061901R (2003).
- [32] S. Turbide, C. Gale, S. Jeon and G. D. Moore, Phys. Rev. C**72**, 014906 (2005).
- [33] J. Kapusta, P. Lichard, and D. Seibert, Phys. Rev. D**44** 2774 (1991).
- [34] C. Y. Wong and H. Wang, Phys. Rev. C**58**, 376 (1998).
- [35] J. F. Owens, Rev. Mod. Phys. **59**, 465 (1987).
- [36] J. Pumplin, D.R. Stump, J. Huston, H.L. Lai, P. Nadolsky, W.K. Tung, J. High Energy Phys. **012** 0207 (2002).
- [37] S. S. Adler et al., Phys. Rev. Lett. **98** 012002 (2007).
- [38] J. F. Owens, Reviews of Modern Physics, Vol-59, No. 2, 465 (1987).